International Journal of Chemical and Biochemical Sciences
(ISSN 2226-9614)

Journal Home page: www.iscientific.org/Journal.html

Decolorization of textile effluent by photo catalytic degradation

M.E. Ossman [a,b*], M. Abdel Fattah [a]

[a] *Petrochemical Eng .Dept., Faculty of Engineering, Pharos University, Alexandria, Egypt*
[b] *City for Scientific Research and Technological Application,(CSAT), Alexandria, Egypt*

Abstract

Many industries such as textiles use dyes in order to colour their products. The presence of these dyes in water even at very low concentration is highly visible and undesirable. Photo catalytic technique offers a good potential to remove colour from waste water. In the present paper g–C3N4 were synthesized by thermal decomposition of mylamine and characterized then employed for removal of methyl orange (MO) and ethylene blue (MB). The operating variables such as adsorbent dose, dye concentration, and pH were studied and the results showed that the optimal conditions for photo-degradation of MO were found to be 0.04 g/L catalyst at a solution pH 7 while the optimal conditions for photo degradation of MB were found to be 0.08 g/L catalyst at a solution pH 9. The kinetics of heterogeneous photo catalysis reactions was studied and the results indicated that found the reaction was found to follow pseudo- first order kinetics and Langmuir–Hinshelwood model described it well. The surface reaction rate constant and Langmuir–Hinshelwood adsorption equilibrium constant for MO were found to be 10.537 (mg/L.min) and 0.004 L/mg. respectively and The surface reaction rate constant and Langmuir–Hinshelwood adsorption equilibrium constant for MB were found to be k = 0.7756 (mg/L.min) and 0.0184 L/mg respectively.

Key words: Graphitic carbon nitride (g-C3N4), Photo catalyst, degradation, Methyle orange, methylene blue

Full length article Received: 23-11-2014 Revised: 04-04-2015 Accepted: 15-04-2015 Available online: 31-05-2015
*Corresponding Author, e-mail: mhr1410@hotmail.com, Phone: 20-100-139-2281

1. Introduction

Heterogeneous photo catalysis represents a promising technology for the degradation of organic pollutants [1]. It presents a 'green' treatment approach; since, toxic organic pollutants are converted into carbon dioxide (CO2), water and mineral acids [2-5]. The heterogeneous photo catalytic reactions occur on the surface of semiconductor according to Langmuir-Hinshelwood mechanism [6, 7]. The removal of environmental pollutions through semi-conductor based photo catalysis has attracted extensive interest over the last several decades, and TiO2 is the most studied semiconductor photo catalyst because of its high photo catalytic activity, low cost, non-toxicity, chemical stability, and biocompatibility [8]. Great effort has been expended toward the development of new visible-light-responsive photo catalysts [9–11]. Recently, graphite-like carbon nitride (C3N4) has emerged as a potential photo catalyst with excellent visible-light photo catalytic activity. Thus, C3N4 has recently been reported to produce hydrogen and oxygen from water splitting and to degrade organic pollutants under irradiation with visible light [12, 13].
Wang et al. reported that g-C_3N_4 with a band gap of 2.7 eV achieved functionality as a stable photo catalyst for H_2 evolution from water under visible light irradiation [14–16]. Covalent carbon nitrides have attracted much attention since the theoretical prediction of their remarkable mechanical and electronic properties of some phases[17, 18], for example, g-C_3N_4 was used as catalyst or carrier due to its excellent stability at an ambient condition[19]. This research intended to develop Kinetic Model for photo catalytic degradation of dye using g-C_3N_4.

2. Material and methods

2.1. Preparation of g-C_3N_4

All chemicals for the synthesis and analysis were commercially available and were used without further treatments. The graphitic C3N4 powder was synthesized by the thermal poly condensation of melamine. Typically, 5 g of melamine was placed in a crucible with a cover and calcined at 500˚C for 4 h in a muffle furnace at a heating rate of 20˚C min^{-1}. The resulting yellow product was collected and ground into a powder for further use.

2.2. Preparation of stock solution of methyl orange

Stock solution of methyl orange has a concentration of 1000 ppm prepared by dissolving 1g of methyl orange in 1 litter of distilled water then use the stock solution to prepare 4 solutions with concentrations of 75 ppm, 100 ppm, 150 ppm and 200 ppm.

2.3. Photo catalytic performance of $C_3H_6N_6$

Photo catalytic activity of C_3N_4 for methyl orange degradation was evaluated in a Pyrex glass beaker with the volume of 250 mL, 0.01g C_3N_4 was dispersed in methyl orange aqueous solution, put the 250mL beaker in 1500mL

beaker contain cooling water as shown in Fig. 1 . Photo degradation of methyl orange was performed under a 300 W U-V lamp with cutoff filter for visible light (256 nm). At an hour interval, and then the concentration of methyl orange was analyzed using the UV – visible spectro photometer at 630 nm.

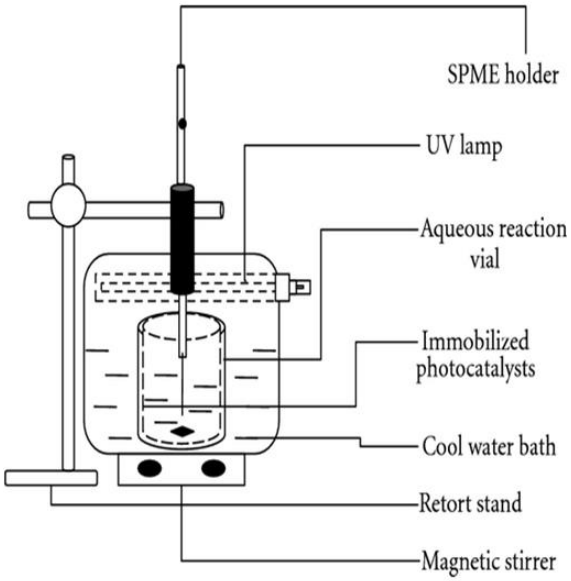

Fig. 1. Apparatus design

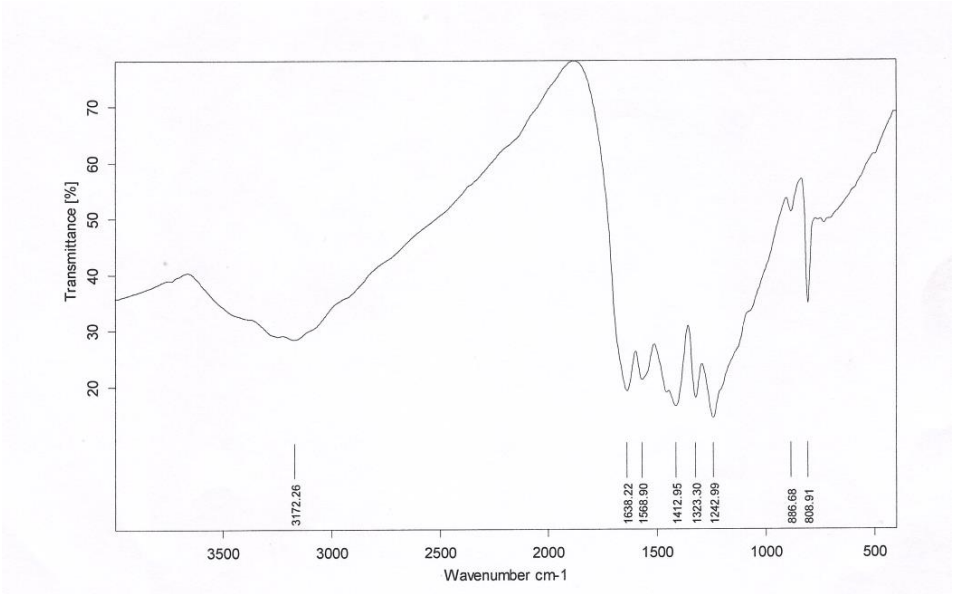

Fig. 2. FTIR for g- C_3N_4

3. Results and discussion:

3.1 Characterization of g-C_3N_4 :

3.1.1. FTIR analysis

The surface functional groups and structure were studied by FTIR spectroscopy. The FTIR spectra of the prepared g- C_3N_4 were recorded between 500 and 4000 cm^{-1} in FTIR- 8400 S Shimadzu. The Fourier transformed infrared (FTIR) spectra of samples are shown in Fig. 2. It can be seen those three regions in the spectra: 808 cm^{-1}, 1242 – 1638 cm^{-1} and 3172 cm^{-1}. It is well known that the bands at 808 cm^{-1} corresponds to the characteristic breathing mode of the triazine units (Fig. 3.). Several strong bands in the 1242 – 1638 cm^{-1} region are the stretching modes of CN heterocyclics [20 – 23]. More than that, the sharp peak at 1683 cm^{-1} can be deemed as an indication of good crystallinity of g- C_3N_4. The two absorption peaks at 1300–1412 cm^{-1} and 1529–1638 cm^{-1} are assigned, respectively, to C(sp^2) –N (1320 cm^{-1}) and C(sp2) =N (1610 cm^{-1}) stretching modes in a graphite-type structure (such a band is forbidden in the FTIR spectrum of pure graphite single crystals). Additionally, a broad band at around 3172 cm^{-1} is indicative of NH stretching vibration modes. Indeed, as reported, the residual hydrogen atoms bind to the edges of the graphene–like C – N sheet in the form of C – NH_2 and 2 C – NH bonds [24].

3.1.2. SEM analysis

In order to know the structure sight of the g- C_3N_4 prepared, Scanning Electron Microscopy (SEM) was employed to visualize sample morphology. In the present work, the g- C_3N_4 prepared was analyzed by using SEM "JEOL JSM 6360LA". The surface morphology of the g-C_3N_4 is presented in Fig. 4. Fig. 4 shows that the samples appeared to have aggregated particles, which contained many smaller crystals and well-crystallized C_3N_4 nanostructures with clear hexagonal morphology and size range of 50–500 nm.

3.2. Effect of contact time

Fig.5 and Fig 6 represent the photo catalytic activities of g-C_3N_4 samples with different concentrations of MO and MB respectively under visible light irradiation. MO and MB concentration very gradually decreased in the presence of g-C_3N_4 under visible light. The absorbance dropped obviously as the irradiation time increased, about 100% MO was photo degraded after irradiation for 1 h using 0.04g/l of g-C_3N_4 while 70% MB was photo degraded after irradiation for 1 h using the same amount of g-C_3N_4. Also it is noticed that increasing the concentrations of both dyes showed lower %removal.

3.3. Effect of Catalyst Dosage

The effect of g-C_3N_4 dosage on the MO and MB removal were studied and the results are shown in Fig. 7 and Fig.8 respectively. The experiments were carried out with a 75 ppm MO dye solution and 10 ppm MB dye solution for 60 min. Fig. 8 shows that the removal efficiency for MB increases with increasing the catalyst dosage.

Fig. 7 and Fig.8 showed that the removal efficiency for MO and MB increased with increasing the catalyst dosage and then stayed nearly constant in a specific catalyst dosage. This is can be explained that the addition of higher quantities of g-C_3N_4 is supposedly increased opacity of the suspension [25,26]. The most effective decomposition of MO was observed at 0.08 g/l of g-C_3N_4

3.4. Effect of Initial Dye Concentration

Fig. 9 and Fig. 10 show the effect of initial concentration of dyes (MO and MB respectively) solutions on the removal percentage at catalyst dosage of 0.04 g/l g-C_3N_4 for 1hr. As expected there is a decrease in the rate of degradation of the dye with an increase in the initial MO and MB concentration. The reason is that when the initial concentration of dye is increased, more and more dye molecules are adsorbed on the surface of g-C_3N_4. Since the existence of the large amounts of adsorbed dye results in the lack of any direct contact with the holes or hydroxyl radicals, this might have an inhibitive effect on the dye degradation. Other possible reasons for these results is the effect of UV screening of the own dye. In high dye concentrations a major amount of UV tends to be absorbed by dye molecules. This reduces the efficiency of the catalytic reaction due to the decline in OH• and OH2• concentrations. Another possible reason is the formation of the by-products during the degradation of mother dye molecules. Moreover the percentage removal decreases rapidly at low MO and MB concentrations and then changes slowly as the initial concentration increases [27-28].

3.5. Effect of solution pH

The effect of pH on the photo degradation of MO in the presence of C_3N_4 represented in Fig. 11 while the effect of pH on the photo degradation of MB represented in Fig. 12 . Fig 11 showed that the photo degradation efficiency of MO solution is strongly affected by changing pH. The highest removal rate of MO was obtained at a pH of 7.0. While for the photo degradation of MB solution; the percentage removal increased from lower to higher as shown in Fig. 11. At strong acidic condition, the percentage removal of MB was 30% while at higher pH, the trend of the removal was increased (70% removal). The results showed good agreement with literature [29].

3.6 Removal kinetics:

Because of the influence of many factors and their mutual effects heterogeneous photo catalysis reactions are complicated processes.

The rate equation can be stated with observed rate constant (k_{obs}) as follows:

$$-r_{\,phenol} = -\frac{dC_{phenol}}{dt} = k_{obs}\ C_{phenol}^{n} \quad (1)$$

The pseudo-first order kinetic model (n=1) provide equation 1 to the following form:

$$-\ln\left(\frac{C_{phenol}}{C_{phenol\,0}}\right) = k_{obs}\,t \quad (2)$$

While for pseudo- second order kinetics model (n=2) provide equation 1 to the following form:

$$\frac{1}{C_{dye}} - \frac{1}{C_{dye\,0}} = k_{obs}\,t \quad (3)$$

Table 1 and Table 2 show lists of the pseudo first order rate constant k_{obs1}, and R^2 for MO and MB respectively while Table 3 and Table 4 show lists of the pseudo second order rate constant k_{obs2}, and R^2. By comparing the R^2, it was found that both MO and MB photo degradation follow pseudo first order kinetic expression.

Many reports have indicated that the kinetic model for heterogeneous photo catalysis follows the Langmuir-Hinshelwood kinetic expression [30].

$$r = -\frac{dC_{phenol}}{dt} = \frac{kK_{phenol}\left[C_{phenol}\right]}{1 + K_{phenol}\left[C_{phenol}\right]} = k_{obs}\, C_{phenol} \quad (4)$$

$$\frac{1}{k_{obs}} = \frac{1}{kK_{phenol}} + \frac{C_{phenol0}}{k} \quad (5)$$

In Eqs. (4) and (5), C_{dye0} is the initial dye concentration (ppm), K_{dye} is the Langmuir-Hinshelwood adsorption equilibrium constant (L/mg), k is the rate constant of the surface reaction (mg/L.min), and k_{obs} is the pseudo first order rate constant. According to Eq. (5), $1/k_{obs}$ versus $[C_{dye0}]$ is a straight line and in this case the rate constant for the surface reaction of MO is k = 10.537 (mg/L.min) and the adsorption equilibrium constant, for MO is K_{dye} = 0.004 L/mg. The obtained regression coefficient R is 0.9807, which suggests that the photo degradation of MO catalyzed by g-C_3N_4 fits the Langmuir- Hinshelwood kinetic model.

The rate expression for photo catalytic degradation of MO using g-C_3N_4 is:

$$r = \frac{0.0382 * \left[C_{dye}\right]}{1 + 0.004 * \left[C_{dye}\right]} \quad (6)$$

While the rate constant for the surface reaction of MB is k = 0.7756 (mg/L.min) and the adsorption equilibrium constant, for MB is K_{dye} = 0.0184 L/mg. The obtained regression coefficient R is 0.9788, which suggests that the photo degradation of MB catalyzed by g-C_3N_4 fits the Langmuir-Hinshelwood kinetic model.

The rate expression for photo catalytic degradation of MB using g-C_3N_4 is:

$$r = \frac{0.01426 * [C_{dye}]}{1 + 0.0184[C_{dye}]} \quad (7)$$

Table 1: Pseudo first order rate constant k_{obs1}, and R^2

MO Concentration (ppm)	k_{obs1} (1/min)	R^2
75	0.0306	0.8774
100	0.0273	0.8419
150	0.0251	0.8468
200	0.0221	0.8382

Table 2: Pseudo first order rate constant k_{obs1}, and R^2

MB Concentration (ppm)	k_{obs1} (1/min)	R^2
10	0.0178	0.9571
20	0.0152	0.9622
30	0.0122	0.916
40	0.0025	0.79

Table 3: Pseudo second order rate constant k_{obs2}, and R^2

MO Concentration (ppm)	k_{obs2} (l/mg.min)	R^2
75	0.0288	0.44
100	0.0009	0.68
150	0.0007	0.696
200	0.0005	0.699

Table 4: Pseudo second order rate constant k_{obs2}, and R^2

MB Concentration (ppm)	k_{obs2} (l/mg.min)	R^2
10	0.0014	0.722
20	0.0015	0.3593
30	0.0018	0.348
40	0.0019	0.48

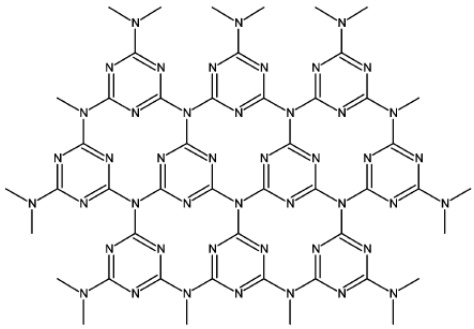

Fig. 3. Triazine- connection patterns of potential g-C_3N_4 allotropes.

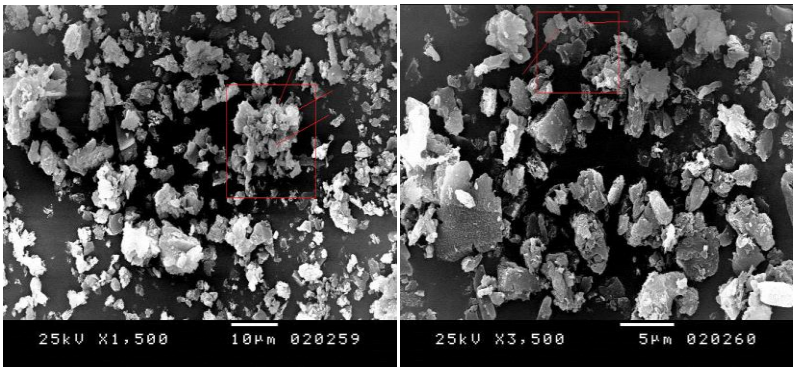

(a) (b)

Fig. 4. The surface morphology of the g- C_3N_4 (SEM).

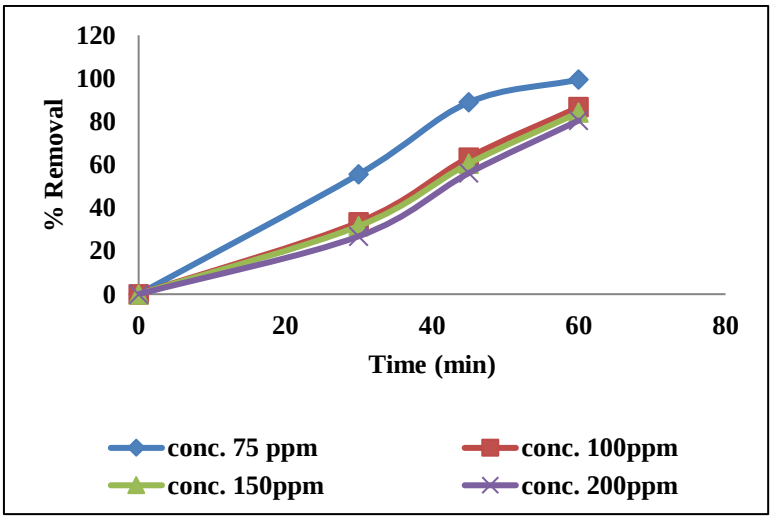

Fig. 5. Removal of MO under visible light irradiation in the presence of g-C_3N_4. (0.04 g/l of g-C_3N_4).

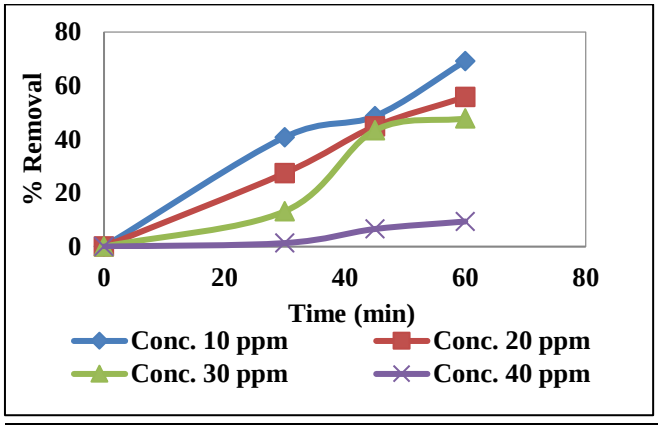

Fig. 6. Removal of MB under visible light irradiation in the presence of g-C_3N_4.(0.04 g/l of g-C_3N_4).

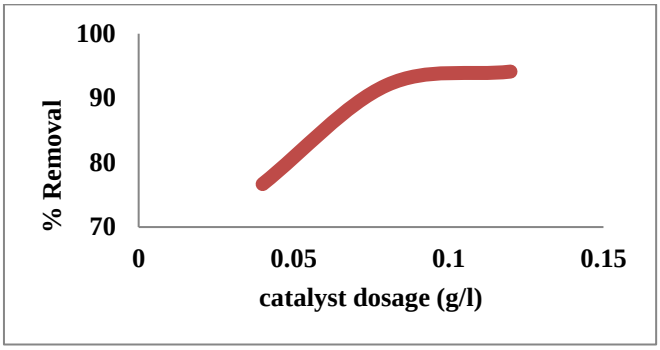

Fig. 7. Effect of dosage of g-C_3N_4 on MO removal. The conc. of dye solution is 100 ppm for 60 min.

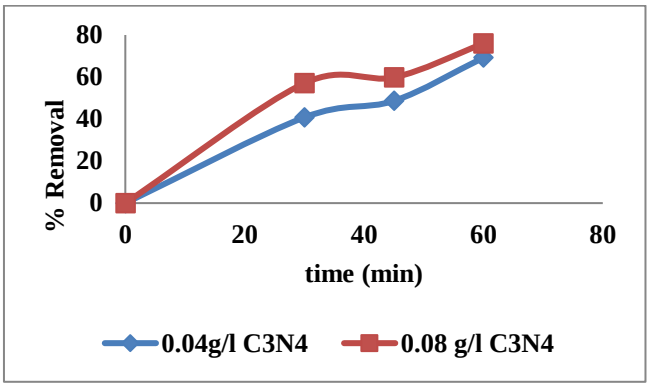

Fig. 8. Effect of dosage of g-C_3N_4 on MB removal. The conc. of dye solution is 10 ppm for 60 min

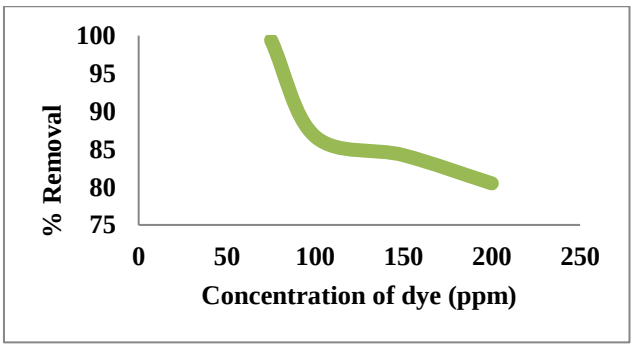

Fig 9. Effect of initial dye concentration on MO removal (0.04 g/l of g-C_3N_4 for 1hr)

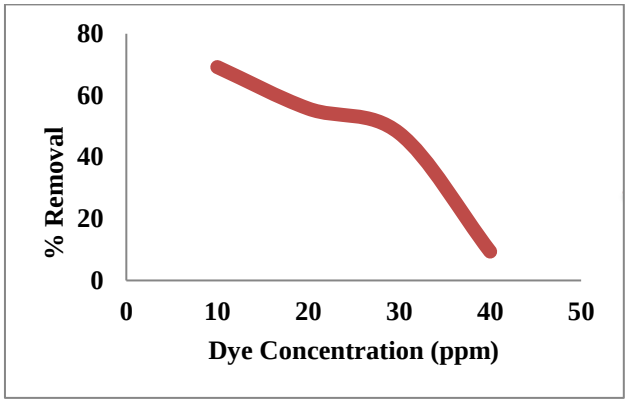

Fig 10. Effect of initial dye concentration on MB removal (0.04 g/l of g-C_3N_4 for 1hr)

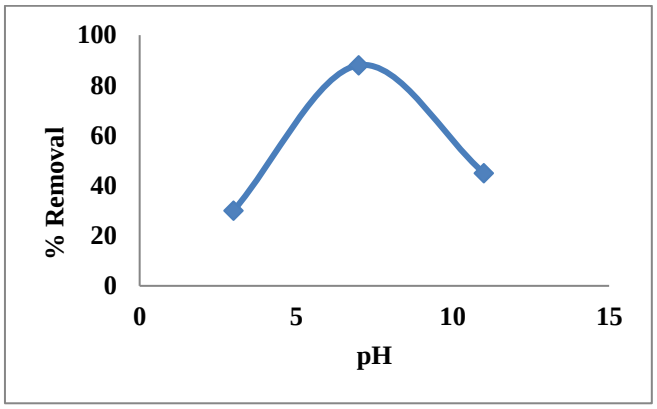

Fig .11. Effect of pH on MO removal for Conc. 100 ppm (0.04 g/l of g-C_3N_4 for 1hr)

4. Conclusion

G-C_3N_4, synthesized by thermal decomposition of mylamine, was found to be efficient as photo catalyst for degradation of MO and MB dye under UV irradiation. The reaction was found to follow pseudo- first order kinetics and Langmuir–Hinshelwood model described it well. The surface reaction rate constant and Langmuir–Hinshelwood adsorption equilibrium constant for MO were found to be 10.537 (mg/L.min) and 0.004 L/mg. respectively and The surface reaction rate constant and Langmuir–Hinshelwood adsorption equilibrium constant for MB were found to be *k* = 0.7756 (mg/L.min) and 0.0184 L/mg respectively. It was observed that degradation of MO and MB is depending on operating parameters, such as, concentration of dye, catalyst dosage and pH. The optimal conditions for photo degradation of MO were found to be 0.04 g/L catalyst at a solution pH 7 while the optimal conditions for photo degradation of MB were found to be 0.08 g/L catalyst at a solution pH 9.

References

[1] Herrmann, J. M.; Guillard, C.; Pichat, P. Heterogenous photo catalysis: an emerging technology for water treatment. *Catal. Today* **1993**, *17*, 7–20.

[2] Hoffmann, M.R.; Martin, S.T.; Choi, W.; Bahnemann D.W. Environmental application of semiconductor photo catalysis. *Chem. Rev.* **1995,** *95*, 69–96.

[3] Mills, A.; Le Hunte, S. An overview of semiconductor photo catalysis. *J. Photochem. Photobiol. A: Chem.* **1997,** *108*, 1–35.

[4] Ollis, D.F.; Turchi, C. Heterogeneous photo catalysis for water purification: Contaminant mineralization kinetics and elementary reactor analysis. *Environ. Prog.* **1990,** *9*, 229–234.

[5] Barka, N.; Qourzal, S.; Assabbane, A.; Nounah, A.; Ait-Ichou, Y. Triphenylmethane dye, patent blue V, photo catalytic degradation on supported TiO2: Kinetics, mineralization and reaction pathway. *Chem. Eng. Com.* **2011,** *198*, 1233–1243.

[6] Barka, N.; Assabbane, A.; Nounah, A.; Aît Ichou, Y. Photo catalytic degradation of indigo carmine in aqueous solution by TiO_2-coated non-woven fibres. *J. Hazard. Mater.* **2008,** *152(3)*, 1054–1059.

[7] [7] Barka, N.; Qourzal, S; Assabbane, A.; Nounah, A.; Aît Ichou, Y. Factors influencing the photo catalytic degradation of Rhodamine B by TiO2-coated non-woven paper. *J. Photochem. Photobiol. A: Chem.* **2008,** *195(2-3)*, 346–351.

[8] Li, F.T., Zhao, Y., Hao, Y.J. , Wang, X.J., Liu, R.H., Zhao, D.S., Chen, D.M., N-doped P25 TiO_2 –amorphous Al_2O_3 composites: one-step solution combustion preparation and enhanced visible-light photo catalytic activity, J. Hazard. Mater. 239–240 (2012) 118–127.

[9] Liu, G. , Zhao, Y.N., Sun, C.H., Li, F., Lu, G.Q., Cheng, H.M., Synergistic effects of B/N doping

on the visible-light photo catalytic activity of mesoporous TiO2, Angew. Chem. Int. Ed. 47 (2008) 4516–4520.

[10] Murakami, N., Takebe, N., Tsubota, T., Ohno, T. , Improvement of visible light Photo catalytic acetaldehyde decomposition of bismuth vanadate/silica nanocomposites by cocatalyst loading, J. Hazard. Mater. 211–212 (2012) 83–87.

[11] Li, F.T., Zhao, Y., Liu, Y., Hao, Y.J., Liu, R.H., Zhao, D.S. , Solution combustion synthesis and visible light-induced photo catalytic activity of mixed amorphous and crystalline MgAl2O4 nanopowders, Chem. Eng. J. 173 (2011) 750–759.

[12] Wang, X.C., Maeda, K., Thomas, A., Takanabe, K., Xin, G., Carlsson, J.M., Domen, K., Antonietti, M., A metal-free polymeric photo catalyst for hydrogen production from water under visible light, Nat. Mater. 8 (2009) 76–82.

[13] Wang, X.C., Maeda, K., Chen, X.F., Takanabe, K., Domen, K., Hou, Y.D., Fu, X.Z., Antonietti, M., Polymer semiconductors for artificial photo synthesis: hydrogen evolution by mesoporous graphitic carbon nitride with visible light, J. Am. Chem. Soc. 131 (2009) 1680–1681.

[14] Chen, X., Jun, Y. S., Takanabe, K., "Ordered mesoporous SBA-15 type graphitic carbon nitride: a semiconductor host structure for photo catalytic hydrogen evolution-with visible light, "Chemistry of Materials, vol. 21, no. 18, pp. 4093–4095, 2009.

[15] [Wang, X. , Maeda, K., Thomas, A., "A metal-free polymeric photo catalyst for hydrogen production from water under visible light," Nature Materials, vol. 8, no. 1, pp. 76–80, 2009.

[16] Maeda, K. , Wang, X., Nishihara, Y., Lu, D., Antonietti, M., and Domen, K., "Photo catalytic activities of graphitic carbon nitride powder for water reduction and oxidation under visible light," Journal of Physical Chemistry C, vol. 113, no. 12, pp. 4940–4947, 2009.

[17] Liu, A. Y., Cohen, M. L.,"Prediction of new low compressibility solids," Science, vol. 245, no. 4920, pp. 841–842, 1989.

[18] Hu, J. M., Cheng, W. D., Huang, S. P., "First-principles modeling of nonlinear optical properties of C_3N_4 polymorphs," Applied Physics Letters, vol. 89, pp. 261117–261119, 2006.

[19] Goettmann, F. , Fischer, A. , Antonietti, M., Thomas, A. , "Chemical synthesis of mesoporous carbon nitrides using hard templates and their use as a metal-free catalyst for Friedel-Crafts reaction of benzene," Angewandte Chemie, vol. 45, no. 27, pp. 4467–4471, 2006.

[20] Komatsu, T., Prototype carbon nitrides similar to the symmetric triangular form of melon. J. Mater Chem, vol. 11, (2001), pp.802-805.

[21] Komatsu, T., "Attempted chemical synthesis of graphite-like carbon nitride," *J Mater Chem*, vol. 11, (2001) , pp. 799-802.

[22] Komatsu, T., "The first synthesis and characterization of cyameluric high polymers," *Macromol Chem Phys*, vol. 202, (2001), pp. 19-25.

[23] Li, X. F., Zhang, J., Shen, L. H., "Preparation and characterization of graphitic carbon nitride through pyrolysis of melamine," *Appl Phys A: Mater Sci Proc*, vol. 94, (2009), pp. 387-392.

[24] Kritikos, D.E., Xekoukoulotakis, N.P., Psillakis, E., Mant-zavinos, D., Photo catalytic degradation of reactive black 5 in aqueous solutions: Effect of operating conditions and coupling with ultrasound irradiation, J. water research. 41, (2007), pp. 2236 – 2246.

[25] Wu, C.H., Chang, H.W., Chern, J., Basic dye decomposition kinetics in a photo catalytic slurry reactor, J. Hazardous Materials. B137, (2006) , pp.336–343.

[26] Banat, F., Al-Asheh, S., Al-Rawashteh, M., Nusair, M., Photo-degradation of methylene blue dye bye the UV/H2O2 and UV/aceton oxidation processes, J. Desalination. 18, (2005), pp. 225-232.

[27] Shimizu, N., Ogino, C., Dadjour, M.F., Murata, T., Sonocata-lytic degradation of methylene blue with TiO2 pellets in water, J. Ultrasonics Sonochemistry. 14, (2007) , pp.184–190.

[28] Barhon, Z. , Saffaj, N., Albizane, A., Azzi, M., Mamouni , R., El Haddad, M. , Effect of Modification of Zirconium Phosphate by Silver on Photo degradation of Methylene Blue, J. Mater. Environ. Sci. 3 (5), (2012),pp. 879-884.

[29] Al-Ekabi H, Serpone N. Kinetic studies in heterogeneous photo catalysis. 1. Photo catalytic degradation of chlorinated phenols in aerated aqueous solutions over TiO_2 suported on a glass matrix, *J. Phys. Chem.*, 1988, 92: 5726.

[30] Morales, G.V. , Sham., E.L., Cornejo, R. , Farfan Torres, E.M. , Kinetic studies of the photo catalytic degradation of tartrazine, Latin American Applied Research, 42(2012), 45-49